HHS Public Access

Author manuscript

Toxicol Appl Pharmacol. Author manuscript; available in PMC 2019 August 15.

Published in final edited form as:

Toxicol Appl Pharmacol. 2018 August 15; 353: 31–42. doi:10.1016/j.taap.2018.06.009.

The tamoxifen derivative ridaifen-B is a high affinity selective CB_2 receptor inverse agonist exhibiting anti-inflammatory and anti-osteoclastogenic effects

Lirit N. Franks[a], **Benjamin M. Ford**[a], **Toshifumi Fujiwara**[b], **Haibo Zhao**[b], and **Paul L. Prather**[a,*]

[a]Department of Pharmacology and Toxicology, College of Medicine, University of Arkansas for Medical Sciences, Little Rock, AR, USA

[b]Department of Internal Medicine, Endocrinology Division, College of Medicine, University of Arkansas for Medical Sciences, Little Rock, AR, USA

Abstract

Selective estrogen receptor modulators (SERMs) target estrogen receptors (ERs) to treat breast cancer and osteoporosis. Several SERMs exhibit anti-cancer activity not related to ERs. To discover novel anti-cancer drugs acting via ER-independent mechanisms, derivatives of the SERM tamoxifen, known as the "ridaifen" compounds, have been developed that exhibit reduced or no ER affinity, while maintaining cytotoxicity. Tamoxifen and other SERMs bind to cannabinoid receptors with moderate affinity. Therefore, ER-independent effects of SERMs might be mediated via cannabinoid receptors. This study determined whether RID-B, a first generation ridaifen compound, exhibits affinity and/or activity at CB_1 and/or CB_2 cannabinoid receptors. RID-B binds with high affinity (K_i = 43.7 nM) and 17-fold selectivity to CB_2 over CB_1 receptors. RID-B acts as an inverse agonist at CB_2 receptors, modulating G-protein and adenylyl cyclase activity with potency values predicted by CB_2 affinity. Characteristic of an antagonist, RID-B co-incubation produces a parallel-rightward shift in the concentration-effect curve of CB_2 agonist WIN-55,212-2 to inhibit adenylyl cyclase activity. CB_2 inverse agonists are reported to exhibit anti-inflammatory and anti-ostoeclastogenic effects. In LPS-activated macrophages, RID-B exhibits anti-inflammatory effects by reducing levels of nitric oxide (NO), IL-6 and IL-1α, but not TNFα. Only reduction of NO concentration by RID-B is mediated by cannabinoid receptors. RID-B also exhibits pronounced anti-osteoclastogenic effects, reducing the number of osteoclasts differentiating from primary bone marrow macrophages in a cannabinoid receptor-dependent manner. In summary, the tamoxifen derivative RID-B, developed with reduced affinity for ERs, is a high affinity selective CB_2 inverse agonist with anti-inflammatory and anti-osteoclastogenic properties.

*Corresponding author at: University of Arkansas for Medical Sciences, College of Medicine, Department of Pharmacology and Toxicology, Slot 611, 4301 West Markham Street, Little Rock, AR 72205, USA. pratherpaull@uams.edu (P.L. Prather).

Conflict of interest disclosure statement

The authors declare that they have no financial or personal conflicts of interest that influenced, or could be perceived to have influenced, this work.

Keywords

Cannabinoid receptors; G-protein coupled receptors; Inverse agonist; Antagonist; Drug action

1. Introduction

Cannabinoids have been used for medicinal purposes for centuries; however, there are only two FDA-approved cannabinoids that are currently used therapeutically (Grotenhermen and Muller-Vahl, 2012). Cannabinoids can be endogenously produced (endocannabinoids), extracted from plants (phytocannabinoids) or synthetically produced (synthetic cannabinoids) (Pertwee, 2006). They act at two major types of receptors, CB_1 and CB_2 receptors, which are $G_{i/o}$-coupled seven transmembrane receptors. Cannabinoids that are FDA-approved for therapeutic use act at both CB_1 and CB_2 receptors (Pertwee, 2010); however, unfortunately produce many adverse effects, including euphoria, lightheadedness, sedation, tolerance and dependence (Clark et al., 2005). Thus, there is a need to develop drugs acting via cannabinoid receptors with fewer side effects.

There is significant scientific evidence supporting the development of drugs that act at either CB_1 or CB_2 receptors. For example, CB_1 receptors are densely expressed in the central nervous system (CNS), making these receptors potential targets for many CNS-related disorders, such as epilepsy, Parkinson's disease, Huntington's disease, pain, nausea and decreased appetite (Pertwee, 2010; Garcia et al., 2011; Valdeolivas et al., 2012). Although CB_2 receptors primarily modulate immune function, they are also expressed in the CNS, reproductive system and bone (Bhutani and Gupta, 2013; Cabral et al., 2015; Hojnik et al., 2015). Drugs acting via CB_2 receptors could prove therapeutically useful for treatment of diseases related to immune function, including inflammatory disorders (Cabral and Griffin-Thomas, 2009) and neuropathic pain (Wilkerson et al., 2012), but also have been shown to produce anti-angiogenic and anti-proliferative effects in several types of cancer (Vidinsky et al., 2012).

Our laboratory and others have recently reported that several selective estrogen receptor modulators (SERMs) exhibit moderate affinity for cannabinoid receptors and act as inverse agonists (Kumar and Song, 2013; Prather et al., 2013; Ford et al., 2016). SERMs are agonists and antagonists at estrogen receptors (ERs) and have traditionally been used therapeutically to treat ER-positive breast cancer, post-menopausal conditions, and osteoporosis (Maximov et al., 2013). Interestingly, some SERMs demonstrate anti-cancer activity in cancers devoid of ERs (Martinkovich et al., 2014). A potential mechanism to explain these ER-independent effects of SERMs might be due to inverse agonist activity at cannabinoid receptors. Thus, development of cannabinoid ligands based on a SERM scaffold might result in efficacious anti-cancer drugs acting via a novel mechanism with reduced side effects. However, to avoid potential ER-related adverse effects, it will first be important to develop SERM-based cannabinoids that act selectively at CB_1 and/or CB_2 receptors and lack affinity for ERs.

Tamoxifen, a SERM in the triphenylethylene class, has been used for decades for treatment of ER-positive breast cancer. However, due to tissue-specific action at ERs not expressed in

breast, tamoxifen also unfortunately produces several adverse effects, including increased incidence of endometrial cancer, stroke, hot flashes, and ocular changes (Maximov et al., 2013; Martinkovich et al., 2014). A class of pseudo-symmetrical derivatives of tamoxifen has been synthesized with the goal of decreasing affinity for ER receptors, to reduce these adverse effects, while maintaining cytotoxic actions in cancer via novel ER-independent mechanisms of action (Shiina et al., 2008; Guo et al., 2013b). This novel class is referred to as the ridaifen (RID) compounds, and a first generation compound, ridaifen-B (RID-B), appears to have promise against some forms of cancer by inhibiting cell proliferation more efficaciously than tamoxifen (Nagahara et al., 2008; Tsukuda et al., 2013). Importantly for this study, RID-B is equally cytotoxic in both ER-positive and ER-negative cancer cells. Furthermore, the mechanism of action of RID-B has been shown to be different from that of tamoxifen, as well as 200 other existing cancer medications (Tsukuda et al., 2013). Since cannabinoids and RID-B share cytotoxicity in several types of ER-negative cancers (Alexander et al., 2009; Nagahara et al., 2013), it is possible that the ER-independent actions of RID-B are mediated via cannabinoids receptors.

As an initial step to determine if cannabinoid receptors may contribute to the effects of RID-B, this study characterized the affinity and activity of RID-B at cannabinoid receptors. Based on our previous studies with other SERMs, it was hypothesized that RID-B exhibits moderate to high affinity for the cannabinoid receptors and demonstrates inverse agonist activity with anti-inflammatory and anti-osteoclastogenic activity.

2. Materials and methods

2.1. Materials

Ridaifen-B, CP-55,940, and JWH-015 were purchased from Sigma Aldrich (St. Louis, MO). WIN-55,212-2, AM-630, and AM-281 were obtained from Tocris Bioscience (Minneapolis, MN). SR-144528 was procured from Cayman Chemicals (Ann Arbor, MI). The radioligand [^{3}H]CP-55,940 (131.4 Ci/mmol) was purchased from Perkin Elmer (Waltham, MA) and [^{35}S]GTPγS (1250 Ci/mmol) from American Radiolabeled Chemicals (St. Louis, MO). All compounds were diluted to 10^{-2}M in 100% DMSO and stored at −20 °C. N-1 napthylethlene, sulfanilamide, and lipopolysaccharide from *E. coli* 0111:B4 were purchased from Sigma Aldrich (St. Louis, MO). ELISA kits to measure levels of mouse TNFα and mouse IL-6 were obtained from R&D systems (Minneapolis, MN). Mouse IL-1α release was quantified by ELISA kits procured from Ray Biotech (Norcross, GA). The WST-1 cell proliferation reagent from CellPro Roche was obtained from Sigma Adrich (St. Louis, MO). Reagents for TRAP staining were purchased from Sigma Aldrich (St. Louis, MO). All other supplies were purchased from Fisher Scientific.

3. Methods

3.1. Animals

Bone marrow was extracted from the tibiae and femora of eight to ten week-old C57/BL6J mice. Animals were maintained according to guidelines of UAMS Institutional Animal Care and Use Committee, animal use protocol number 3661.

3.2. Cell culture

Chinese hamster ovary (CHO-K1) cells stably expressing human CB_1 receptors (CHO-hCB_1) were purchased from the DiscoverRx Corporation (Fremont, CA). CHO-K1 cells stably expressing human CB_2 receptors (CHO-hCB_2) were produced in our laboratory as described previously (Shoemaker et al., 2005a). CHO-hCB_1 cells were cultured in Kaighn's modification of Ham's F-12 media (Sigma Aldrich, St. Louis, MO) while Dulhecco's Modification of Eagles's Medium (DMEM; Cellgro, Manassas, VA) was used for CHO-hCB_2 cells. Both types of growth medium contained 10% FetalPlex animal serum complex (Gemini Bio Products, West Sacramento, CA) and 1% penicillin/streptomycin (10,000 IU/ml penicillin, 10,000 μg/ml streptomycin; Cellgro, Manassas, VA) and 0.5 mg/ml of G418 geneticin (Sigma Aldrich, St. Louis, MO), a selection antibiotic used to maintain the stable expression of transfected receptors. Cells were used between passages 4–18 and were maintained in a humidified incubator at 37 °C with 5% CO_2. Cells were harvested using PBS (10mM)/EDTA (1 mM) upon reaching 90–100% confluency. Cells were then either plated for assessment of adenylyl cyclase activity (see following for complete Methods), frozen at −80 °C for future membrane preparation or reseeded into flasks for further culturing of the cell line.

3.3. Membrane preparation

Cell pellets were harvested from CHO cells stably expressing human CB_1 and CB_2 receptors (CHO-hCB_1 and CHO-hCB_2) and stored in −80 °C. Pellets were thawed on ice, pooled and suspended in ice-cold homogenization buffer (50 mM HEPES pH 7.4, 3 mM $MgCl_2$, and 1 mM EGTA). Suspended pellets were placed in a 40 ml Dounce glass homogenizer and subjected to 10 strokes followed by centrifugation at 40,000 × *g* for 10 min at 4 °C. Supernatants were discarded and the homogenization-centrifugation steps were repeated twice more. Pellets were then resuspended with ice-cold 50 mM HEPES, pH 7.4 and aliquoted for storage at −80 °C. Protein concentration was determined using the BCA™ Protein Assay (Thermo Scientific, Rockford IL).

3.4. Competition receptor binding

Increasing concentrations of RID-B (10^{-10} to 10^{-5}M) were co-incubated with 0.2 nM of the CB_1/CB_2 agonist [^{3}H] CP-55,940 as previously reported (Prather et al., 2013). Each sample also contained 50 μg of CHO-hCB_1 or CHO-hCB_2 membrane homogenates, 5 mM $MgCl_2$ and an incubation mix containing 50 mM Tris-HCl buffer (pH 7.4) with 0.05% bovine serum albumin. Nonspecific binding was defined as radioactivity remaining in the presence of 1 μM of non-radioactive CB_1/CB_2 agonist WIN-55,212-2. Assays contained a final volume of 1 ml and were conducted in triplicate. To achieve equilibrium, samples were incubated for 15 min at 37 °C. Termination of reactions was achieved by rapid vacuum filtration through Whatman GF/B glass fiber filters followed by four washes of four mls of ice-cold filtration buffer (50 mM Tris, pH 7.4 and 0.05% bovine serum albumin). Filters were then placed in scintillation vials containing four mls of ScintiverseTM BD Cocktail scintillation fluid (Fisher Scientific, Pittsburg, PA). After overnight incubation in scintillation fluid, radioactivity was quantified by a liquid scintillation spectrophotometer (TriCarb 2100TR Liquid Scintillation Analyzer, Packard Instrument Company, Meriden, CT).

3.5. [^{35}S]GTPγS binding

[^{35}S]GTPγS binding was conducted as described previously (Prather et al., 2013) in a final volume of 1 ml by incubating 25 μg of CHO-hCB_2 membrane homogenates with increasing concentrations of RID-B (10^{-10} to 10^{-5}M) and 0.1 nM [^{35}S]GTPγS in 20mM HEPES buffer containing 10 mM $MgCl_2$, 100 mM NaCl, 10 μM GDP, 0.1% bovine serum albumin. Non-specific binding was defined by radioactivity remaining in the presence of 10 μM of non-radioactive GTPγS. Each assay condition was conducted in triplicate and reactions were incubated for 30 min at 30 °C. Termination of reactions was achieved by rapid vacuum filtration through Whatman GF/B glass fiber filters followed by four washes of four mls of ice-cold filtration buffer (50 mM Tris, pH 7.4 and 0.05% bovine serum albumin). Filters were then placed in scintillation vials containing four mls of ScintiverseTM BD Cocktail scintillation fluid (Fisher Scientific, Pittsburg, PA). After overnight incubation in scintillation fluid, radioactivity was quantified by a liquid scintillation spectrophotometer (TriCarb 2100TR Liquid Scintillation Analyzer, Packard Instrument Company, Meriden, CT).

3.6. Adenylyl cyclase activity

CHO-hCB_2 cells, between the passages of 6–18, were seeded into 24-well plates at a density of 6×10^6 cells per plate and allowed to adhere overnight in a humidified incubator maintained at 37 °C with 5% CO_2. Growth media was then replaced with an incubation media containing DMEM with 0.9 g/l NaCl, 2.5μCi/ml of [^{3}H]adenine and 0.5 mM isobutyl-methyl-xanthine (IBMX) for 3 h. The incubation media was then removed and replaced with 0.5 ml of test compounds in a Krebs-Ringer-HEPES solution (10 mM HEPES, 110 mM NaCl, 25 mM Glucose, 55 mM Sucrose, 5mM KCl, 1 mM $MgCL_2$, and 1.8 mM $CaCl_2$ at pH 7.4) containing 0.5 mM IBMX and 10 μM forskolin. Plates were then floated in a 37 °C water bath for 15 min followed by termination of reactions by adding 50 μl of 2.2 N HCl to each well. [^{3}H]cAMP was collected in 4 ml of final eluate following alumina column chromatography. Following 10 ml addition of ScintiverseTM BD Cocktail scintillation fluid, radioactivity was quantified by a liquid scintillation spectrophotometer (TriCarb 2100TR Liquid Scintillation Analyzer, Packard Instrument Company, Meriden, CT).

In experiments to determine if RID-B acted as a CB_2 antagonist, CHO-hCB_2 cells were first incubated with RID-B (3 μM) for 30 min at room temperature. Following RID-B pretreatment, cells were co-incubated with increasing concentrations (10^{-10} to 10^{-5}M) of the CB_1/CB_2 agonist WIN-55,212-2 for an additional 7 min at room temperature. Reactions were terminated by addition of 50 μl of 2.2 N HCl to each well and samples were processed as described above to isolate and quantify [^{3}H]cAMP.

3.7. Nitric oxide production

Nitric oxide production was quantified by use of the Greiss Reagent. Specifically, RAW 264.7 cells were plated at a density of 10,000 cells per well in DMEM (10% FetalPlex and 1% penicillin/streptomycin) and allowed to adhere overnight in a 37 °C incubator with 5% CO_2. Growth media was removed and replaced with media containing the experimental compounds for 90 min at 37 °C. LPS (concentrations optimized per experiment) was then added and cells incubated for 48 h. Following LPS exposure, 100 μl of media from each well

was removed and added to separate wells of a 96 well plate, to which 150 μl of Greiss reagent (4 mM N-1 napthylethlene, 4% 12.2 N HCl and 46 mM sulfanilamide) was added. Plates were covered with aluminum foil to protect from the light and gently shaken for 15 min and read at 540 nM in a SpectraMax® Plus Spectrophotometer (Molecular Devices Corporation, Sunnyvale, CA). Nitric oxide concentrations were quantified from standard calibration curves containing sodium nitrite concentrations ranging from 0.5 μM to 100 μM.

3.8. Cell viability

Cell viability was assessed by quantifying cellular metabolic activity of RAW264.7 mouse macrophage cells with the cell proliferation WST-1 reagent (CellPro-Ro Roche; Sigma-Adrich, St. Louis, MO). Following indicated drug treatments, growth media was removed and 100 μl of DMEM (10% FetalPlex, 1% penicillin-streptomycin) at 37 °C was added to each well, followed by WST-1 reagent (10 μl). After thorough mixing, cells were incubated at 37 °C with 5% CO_2 for 2–3 h and colormetric differences were quantified by reading absorbance was 450 nM in a SpectraMax® Plus spectrophotometer (Molecular Devices Corporation, Sunnyvale, CA). All values were normalized to percent of vehicle-treated controls.

3.9. Enzyme-linked immunosorbent assays (ELISAs)

Production of mouse TNF-α, IL-1α and IL-6 was quantified by ELISA assays. Specifically, RAW264.7, were pre-incubated with cannabinoid compounds for 1 h prior to addition of 500 ng/ml lipopolysaccharide (LPS) for an additional 48 h incubation. Media was removed and stored at −20 °C. All ELISAs were performed according to the manufacturer's instructions.

3.10. Osteoclast differentiation

Primary bone marrow macrophages were prepared as described previously (Zhou et al., 2015). Briefly, whole bone marrow was isolated from the tibiae or femurs of 8–10 week old mice (C57/BL6J). 5×10^6 Bone marrow cells were then plated in a 10 mm bacteria petri-dish in α-10 medium [α-MEM, 1 × penicillin-streptomycin-L-glutamine solution (Sigma-Aldrich, St. Louis, MO), 10% heat-inactivated fetal bovine serum (Hyclone; GE Healthcare Life Sciences, Pittsburg, PA)], containing a 1/10 volume of M-CSF conditioned medium supernatant (CMG), which is equivalent of 1 μg/ml of M-CSF. Cells were subsequently incubated at 37 °C with 95% O_2 and 5% CO_2 for 4–5 days to generate bone marrow macrophages. During the incubation, fresh media and CMG were replaced every other day. Bone marrow macrophages were then plated into 48 well plates at a concentration of 1.5×10^4 cells/well. For differentiation into osteoclasts, fresh media was replaced on days 2 and 3 containing 1/100 volume of CMG and 100 ng/ml of RANKL. Drug treatments were added on days 2 and 3 and cells were fixed on day 4 with 4% paraformaldehyde in phosphate buffered saline for 20 min, followed by two 5 min washes with phosphate buffered saline. Plates were then stored at 4 °C until tartrate-resistant acid phosphatase staining was performed.

3.11. Tartrate-resistant acid phosphatase (TRAP) staining

As described in (Zhou et al., 2015), bone marrow macrophages were cultured in 48-well culture plates for 4 days in α-10 medium containing M-CSF and RANKL. Afterwards, 4% paraformaldehyde/phosphate buffered saline (PBS) was used to fix the cells. TRAP was then stained using sodium potassium tartrate and napthol AS-BI phosphoric acid. The solution was gently mixed and 0.4 ml added to each well of fixed osteoclasts. After a 20 min incubation at 37 °C, the reactions were terminated by washing with tap water three times and air-dried. TRAP-stained osteoclasts were then quantified visually by microscopy using a grid-system.

3.12. Statistical analyses

GraphPad Prism® v6.0 g (GraphPad Software, Inc.; San Diego, CA) was used for all statistical analyses and curve-fitting. Non-linear regression for one-site competition was used to determine the IC_{50} for competition receptor binding. The Cheng-Prusoff equation (Cheng and Prusoff, 1973) was used to convert the experimental IC_{50} values to K_i values, a quantitative measure of receptor affinity. Similarly, non-linear regression was also used to determine IC_{50}, EC_{50}, E_{max} and I_{max} values for measures of intrinsic activity. Statistical comparison of three or more treatment groups was accomplished by employing one-way ANOVA followed by Dunnett's *post-hoc* comparisons of individual groups.

4. Results

Based on the structural similarity of RID-B to tamoxifen (Fig. 1), and our past reports that tamoxifen exhibits moderate affinity for cannabinoid receptors (Prather et al., 2013; Ford et al., 2016), a competition receptor-binding screen was conducted. From this initial binding screen, it was observed that RID-B (1 μM) produced > 50% displacement of the CB_1/CB_2 radioligand [^{3}H]-CP-55,940 (0.2 nM) from human CB_1 and CB_2 receptors stably expressed in CHO cells. These data suggested that RID-B exhibits sub-micromolar affinity for both cannabinoid receptors (data not shown). As such, subsequent studies were conducted to determine the specific affinity (K_i) of RID-B at both CB_1 and CB_2 receptors (Fig. 2A). Although RID-B exhibits moderate affinity for CB_1 receptors (filled squares) with a K_i value of 732 ± 168 nM (N = 3), this tamoxifen derivative hinds to CB_2 receptors (open squares) with high affinity (e.g., K_i = 43.7 ± 14.6 nM, N = 3). Based on these results, RID-B exhibits 17-fold higher affinity for CB_2 receptors when compared to CB_1 receptors. These data suggest that RID-B is the first SERM-based cannabinoid reported that exhibits moderate CB_2 selectivity. Based on these observations, the focus of subsequent experiments was to characterize CB_2 signaling produced by RID-B.

Experiments were next designed to determine the intrinsic activity of RID-B at CB_2 receptors (e.g., whether RID-B acts as an agonist, antagonist, or inverse agonist). Cannabinoid receptors are coupled to the G_i/G_o subtype G-proteins, thus agonists activate G-proteins, antagonists have no effect, and inverse agonists decrease G-protein activity produced by constitutively active receptors (Pertwee, 2006). The ability of RID-B to modulate G-protein activation was examined by employing a non-hydrolyzable radioactive analogue of GTP, [^{35}S]GTPγS, which hinds to G-proteins irreversibly when activated. As

expected, the well characterized full CB_2 agonist CP-55,940 increases G-protein activation (E_{max} = 25.4 ± 3.0%) with a potency (EC_{50}) of 2.3 ±1.1 nM, *N* = 3 (Fig. 2B). In marked contrast, RID-B decreases G-protein activation below basal levels (I_{max} = −31.2 ± 0.37%) with a potency (IC_{50}) of 300 ± 34 nM (*N* = 3). RID-B has no effect on G-protein activity in CHO cells devoid of CB_2 receptors (data not shown). Collectively, these data indicate that RID-B acts as an inverse agonist at CB_2 receptors for modulation of G-protein activity (Bouaboula et al., 1997).

To provide a second measure of intrinsic activity, CB_2 regulation of adenylyl cyclase activity was examined. Through coupling to G_i/G_o-proteins, CB_2 receptor agonists inhibit the activity of the intracellular effector adenylyl cyclase, resulting in a reduction of intracellular cAMP levels. Neutral antagonists at CB_2 receptors do not affect adenylyl cyclase activity, while inverse agonists increase cAMP levels due to inhibition of constitutively active CB_2 receptors. Consistent with modulation of G-protein activity (Fig. 2B) and also characteristic of an inverse agonist, RID-B increases adenylyl cyclase activity in a concentration-dependent manner, elevating cAMP levels with an I_{max} of 398 ± 30% and a potency (IC_{50}) of 134 ± 397 nM (*N* = 3) (Fig. 2C). RID-B does not alter intracellular cAMP levels in CHO cells not expressing cannabinoid receptors (data not shown). To provide additional evidence for inverse agonist/antagonist action of RID-B at CB_2 receptors, an antagonist dissociation constant (K_b) was determined for RID-B (Fig. 2D). This was accomplished by co-incubating a receptor saturating concentration of RID-B (3 μM) in the presence of increasing concentrations of the full CB_1/CB_2 agonist WIN-55,212-2. As expected, WIN-55,212-2 decreases cAMP level with an efficacy (I_{max}) of 86 ± 2.6% and a potency (IC_{50}) of 0.5 ± 0.3 nM (N = 3) (open triangles). RID-B co-incubation (filled triangles) produces an 11.2-fold decrease in the potency, but not efficacy, of inhibition of adenylyl cyclase activity by WIN-55,212-2 (e.g., resulting in a parallel-rightward shift in the concentration-effect curve), yielding a K_b value of 294 nM ± 67.4 (*N* = 3). In summary, the in vitro pharmacological characterization presented (Fig. 2A–D) clearly indicates that the tamoxifen derivative RID-B acts as a high affinity, selective, inverse agonist at CB_2 receptors when considering modulation of G-protein and adenylyl cyclase activity.

Evidence suggests that CB_2 inverse agonists might be developed therapeutically for use in inflammation and osteoporosis, specifically due to anti-inflammatory (Turcotte et al., 2016) and anti-ostoeclastogenic (Idris et al., 2008; Yang et al., 2013) effects. As such, subsequent experiments were conducted to examine RID-B modulation of inflammatory markers in LPS-activated RAW264.7 macrophages and osteoclast differentiation of primary bone marrow macrophages (e.g., osteoclastogenesis).

To examine potential anti-inflammatory effects of RID-B, nitric oxide (NO) production (a measure of oxidative stress and inflammation (Coleman, 2001)) was first measured following activation of RAW264.7 murine macrophages with increasing concentrations (5–500 ng/ml) of lipopolysaccharide (LPS) for 48 h (Fig. 3). As shown in Fig. 3A, LPS produces a concentration-dependent increase in NO production (as measured by nitrite present in the media) with a potency (ED_{50}) of 77.7 ± 1.4 nM and an efficacy (E_{max}) of 25.0 ± 4.0 (*N* = 5) μM. Consistent with anti-inflammatory properties, co-incubation of LPS with RID-B (300 nM, 500 nM, and 1 μM) significantly decreases the E_{max} of NO production to

19.4 ± 3.8 (N = 3), 22.0 ± 9.9 (N = 3), and 18.2 ± 4.7 (*N* = 4) μM, respectively. RID-B co-incubation did not alter the EC_{50} values of LPS, indicative of non-competitive antagonism.

To determine if cannabinoids receptors participate in the anti-inflammatory actions produced by RID-B in RAW264.7 macrophages, receptor-saturating concentrations of selective and non-selective CB_1 and/or CB_2 agonists and antagonists/inverse agonists were co-incubated with 1 μM of RID-B (a concentration of RID-B that produced maximal reduction in NO production, Fig. 3B). Similar to data presented from the concentration-effect experiments (Fig. 3A), RID-B (1 μM) alone reduced NO production by 30.1 ± 5.1% (*N* = 10) when compared to cells treated only with LPS (500 ng/ml) for 48 h. While producing slight but insignificant effects, co-incubation with selective CB_2 antagonists/inverse agonists AM-630 (5 μM) and SR-144528 (5 μM) (Ross et al., 1999; Rhee and Kim, 2002), or the CB_1 antagonist/inverse agonist AM-281 (5 μM) (Cosenza et al., 2000), did not alter NO levels compared to RID-B administered alone. Interestingly, co-incubation with the selective CB_2 agonist JWH-015 (5 μM) (Murataeva et al., 2012) significantly increases the effect of RID-B, reducing NO levels to 51.1 ± 6.4% (*N* = 4). Importantly, co-incubation with the well characterized non-selective full CB_1/CB_2 agonist CP-55,940 (2 μM) significantly attenuates the anti-inflammatory effect of RID-B, resulting in NO reduction of only 9.3 ± 4.6% (N = 10). Although slight reductions in NO concentrations are observed when cannabinoid agonists or antagonist/inverse agonists are administered alone, none of these effects are significant (white bars).

To examine additional mediators of inflammation in LPS-activated RAW264.7 macrophages, the effect of RID-B on the release of the inflammatory cytokines IL-1α, IL-6 and TNF-α was measured (Fig. 4). In RAW264.7 macrophages treated with LPS (500 ng/ml) for 48 h, IL-1α concentrations are increased to 153.3 ± 16.6 pg/ml (*N* = 4) (Fig. 4A). Indicative of an anti-inflammatory action, RID-B reduces IL-1α levels in a concentration-dependent manner to 73.1 ± 4.7 pg/ml (52.3%) when tested at 1 μM. Co-incubation of RID-B (1 μM) with receptor saturating concentrations of selective CB_2 antagonists/inverse agonists AM-630 (5 μM) and SR-144528 (5 μM), the CB_1 antagonist/inverse agonist AM-281 or the CB_1/CB_2 agonist CP-55,940 (2 μM), does not alter the anti-inflammatory effect of RID-B. No cannabinoid agonist or antagonist/inverse agonist altered IL-1α concentrations when administered alone (white bars).

Consistent with observations for IL-1α, treatment with LPS (500 ng/ml) for 48 h increases IL-6 levels to 636.1 ± 38.01 pg/ml (N = 4), and this increase is reduced by 45% by co-incubation with RID-B (1 μM) to 349.9 ± 34.9 pg/ml (N = 4) (Fig. 4B). Also similar to experiments with IL-1α, co-incubation with all cannabinoid agonists or antagonists/inverse agonists fails to attenuate the anti-inflammatory effect of RID-B on IL-6 release. Curiously, while all other cannabinoids ligands have no effect on IL-6 levels when administered alone, the selective CB_1 antagonist/inverse agonist AM-281 increases IL-6 levels to 1040 ± 119.4 pg/ml (*N* = 4) (white bars).

Finally, TNF-α levels dramatically increase to 17.2 ± 0.48 ng/ml (N = 4) in RAW264.7 macrophages exposed to LPS (500 ng/ml) for 48 h (Fig. 4C). Interestingly, unlike that observed for IL-1α and IL-6, RID-B (1 μM) produces a slight but non-significant increase in

TNF-α levels. However, co-incubation of RID-B with the selective CB_2 antagonist/inverse agonist AM-630 and selective CB_1 antagonist/inverse agonist AM-281 significantly increases TNF-α levels, while co-incubation with the CB_2 agonist JWH-015 or CB_1/CB_2 agonist CP-55,940, have no effect. AM-281, but no other cannabinoids ligands examined, significantly increases TNF-α levels to 21.3 ± 0.21 ($N = 4$) ng/ml when administered alone (white bars).

Collectively, results from studies employing LPS-activated RAW264.7 macrophages suggest that, similar to previous reports for CB_2 inverse agonists (Turcotte et al., 2016), RID-B exhibits anti-inflammatory effects characterized by reduction of oxidative stress and decreased release of inflammatory cytokines. However, the participation of cannabinoid receptors in these responses is complex.

RID-B was designed to exhibit selective cytotoxicity toward cancer cells. Therefore, to assure that the observed reductions in NO production and cytokine levels in the present experiments did not result from cytotoxic actions of RID-B or the other cannabinoids ligands examined, cell viability of RAW264.7 macrophages was assessed in response to the conditions and drug treatments that were employed (Fig. 5). Cell viability of RAW264.7 macrophages was quantified by measuring mitochondrial activity via employing the WST-1 reagent. Forty-eight hour exposure to LPS (500 ng/ml) in the absence or presence of all cannabinoid ligands, examined alone or in combination with RID-B (1 or 3 μM), has no effect on cell viability (Fig. 5A). However, as observed in Fig. 5B, when cells are exposed to higher concentrations of RID-B (10 μM) alone during a 4 h exposure to LPS, cell viability is decreased by 34.0 ± 5.4% ($N = 4$). Interestingly, RID-B cytotoxicity is attenuated by co-incubation with the selective CB_1 antagonist/inverse agonist AM-281 or the CB_1/CB_2 agonist CP-55,940, indicating a potential cannabinoid receptor-mediated mechanism.

A second area of interest for drug development of CB_2 inverse agonists is for potential use in osteoporosis, specifically due to reported anti-ostoeclastogenic (Idris et al., 2008) effects. Osteoclasts are derived from the monocyte/macrophage lineage of hematopoietic stem cells, and overactivity of this modulator of bone plays an important role in development of osteoporosis. To examine the effect of RID-B on osteoclastogenesis, drugs were added to primary bone marrow-derived macrophages in the pre-osteoclast stage, and their development into mature osteoclasts was quantified (Figs. 6 and 7). Pre-osteoclasts exposed only to vehicle matured into 339.1 ± 15.6 (N = 4) osteoclasts per well (Fig. 6A). RID-B produces a concentration-dependent reduction in the number of osteoclasts, resulting in a maximal decrease of 48.6% (174.4 ± 19.2, N = 4) when tested at 300 nM (Figs. 6A and 7B). To determine if the anti-osteoclastogenic effect of RID-B involves cannabinoid receptors, pre-osteoclasts were co-incubated with RID-B (300 nM) and receptor-saturating concentrations of selective and non-selective CB_1 and/or CB_2 agonists and antagonists/inverse agonists (Fig. 6B, 7D and F). Treatment of pre-osteoclasts with the selective CB_2 inverse agonist AM-630 alone reduces osteoclastogenesis to levels similar to that produced by RID-B (168.1 ± 15.4, N = 4) (Fig. 6B and 7C), and in an additive manner following co-incubation with RID-B (94.6 ± 15.6, N = 4) (Figs. 6B and 7D).

Although the CB_2 agonist JWH-015 and CB_1 antagonist/inverse agonist AM-281 also significantly reduce osteoclast development when administered alone, co-incubation has little consequence on the effects of RID-B. Importantly, although the CB_1/CB_2 agonist CP-55,940 marginally reduced osteoclast formation when administered alone (Figs. 6B and 7E), co-incubation significantly attenuated the anti-osteoclastogenic effects produced by RID-B (Fig. 6B and 7F). To summarize, experiments examining osteoclastogenesis indicate that, similar to that reported for other selective CB_2 inverse agonists (Ouyang et al., 2013; Yang et al., 2013), RID-B exhibits significant anti-osteclastogenic effects that may be mediated in part by CB_1 and/or CB_2 receptors.

5. Discussion

The present study identifies RID-B as the first high affinity, selective, CB_2 inverse agonist derived from a SERM scaffold. Furthermore, similar to that reported for other selective CB_2 inverse agonists (Idris et al., 2008; Yang et al., 2013; Reiner et al., 2014; Feng et al., 2015; Presley et al., 2015a), RID-B exhibits anti-inflammatory, anti-osteoclastogenic and cytotoxic effects that are mediated in part by CB_2 and/or CB_1 receptors. RID-B is a first generation pseudo-symmetrical derivative of tamoxifen with reduced ER affinity (Shiina et al., 2008; Guo et al., 2013b), while exhibiting increased affinity for cannabinoid receptors (this study). Collectively, these observations provide proof of principle for development of a novel class of SERM-based cannabinoids that act selectively at CB_2 and/or CB_1 receptors and lack affinity for ERs.

Increasing evidence indicates that CB_2 inverse agonists show promise for development as a novel class of anti-inflammatory drugs (Ueda et al., 2005; Maekawa et al., 2006; Ueda et al., 2007; Lunn et al., 2008). Nitric oxide (NO) (Coleman, 2001) and cytokines (Holdsworth and Gan, 2015) are synthesized and released during inflammatory responses by a variety of immune modulating cell types. Therefore, in the present study, potential anti-inflammatory activity of RID-B was assessed by quantifying the modulation of NO and inflammatory cytokine production in LPS-activated RAW264.7 macrophages. RID-B reduced NO accumulation in macrophages exposed to LPS; however, determining a potential mechanistic role for CB_2 and/or CB_1 receptor involvement in mediating this anti-inflammatory response was complex. For example, although co-incubation of RID-B with the CB_1/CB_2 agonist CP-55,940 significantly attenuates reduction in NO levels produced by RID-B, there is no consistent pattern observed when RID-B is co-incubated with individual cannabinoid agonists or antagonists/inverse agonists that act selectively at CB_1 and/or CB_2 receptors. An obvious explanation for these observations might be that both CB_1 and CB_2 receptors participate in the mechanism by which RID-B reduces NO accumulation in this model, and thus concurrent occupation of both receptors must be achieved to observe antagonism. However, it might also be expected that co-incubation with a CB_2 selective agonist (e.g., JWH-015) would attenuate the effects of a CB_2 inverse agonist/antagonist (e.g., RID-B). Although such reversal was not observed in the present study, these results might be explained by “functional selectivity” often reported for ligands that act at CB_2 receptors (Shoemaker et al., 2005b; Yao et al., 2006; Bosier et al., 2010; Brailoiu et al., 2014; Dhopeshwarkar and Mackie, 2016). The intrinsic activity of functionally selective CB_2 ligands can vary, depending on the cell, tissue and/or signaling pathway examined (Kenakin

and Miller, 2010; Goupil et al., 2012). For example, in transfected cells stably expressing CB_2 receptors, the previously classified CB_2 inverse agonist SR144528 acts as an inverse agonist for regulation of both adenylyl cyclase activity and arrestin recruitment; however, other reported CB_2 inverse agonists AM630 and JTE907 modulate only adenylyl cyclase activity as inverse agonists, but instead act as partial agonists for recruitment of arrestin (Dhopeshwarkar and Mackie, 2016). Therefore, it has not been established whether the cannabinoid ligands used for co-incubation with RID-B in this study, that have been classified as “agonists” or “antagonists/inverse agonists” in other systems, truly exhibit the expected intrinsic activity concerning modulation of pathways involved in NO production in this inflammatory model. Finally, it is also certainly possible that the anti-inflammatory mechanism of action for RID-B in this model is cannabinoid-independent, and might occur via action of RID-B at ERs (see following discussion).

CB_2 inverse agonists also exhibit anti-inflammatory effects via modulation of cytokine release (Reiner et al., 2014; Presley et al., 2015b). In this study, release of pro-inflammatory cytokines IL-6, IL-1α, and TNF-α was examined in LPS-activated macrophages. Consistent with anti-inflammatory actions, RID-B decreases levels of IL-1α and IL-6; however, no effect on TNF-α is observed. Co-incubation with selective CB_1 and/or CB_2 cannabinoid agonists or antagonists/inverse agonists fail to alter reduction of cytokine levels produced by RID-B, indicating that cannabinoid receptors likely do not mediate this antiinflammatory effect. These apparent cannabinoid-independent anti-inflammatory effects of RID-B may involve action at ERs. For instance, although the affinity of RID-B for ERs is lower than tamoxifen (from which it was derived), this analogue nevertheless retains moderately high affinity for ERs (Guo et al., 2013b). Several SERMs, including tamoxifen and raloxifene, exhibit anti-inflammatory activity by reducing oxidative stress and pro-inflammatory cytokine levels in the brain and blood of ovariectomized rats (Yazgan et al., 2016). Raloxifene has also been reported to decrease NO and IL-6 levels in an inflammatory mouse model of Parkinson’s disease (Poirier et al., 2016). Finally, certain xenoestrogens decrease IL-6 release (Teixeira et al., 2016). Collectively, these observations suggest that the cannabinoid-independent reduction in cytokine release observed for RID-B in this study is likely mediated via ERs. Although use of selective ER antagonists might help tease out ER versus CB_2-mediated effects of RID-B on LPS-treated macrophages observed here, a more definitive answer could be provided by development and examination of SERM-based cannabinoids that lack any ER affinity. These studies are ongoing in our laboratory.

It is interesting that RID-B selectively reduces LPS-induced production of interleukins, but not TNFα in RAW 264.7 macrophages. However, it should be noted that selective effects on individual cytokines similar to those reported here have been demonstrated for other CB_2 inverse agonists. For example, the CB_2 inverse agonist SMM-189 reduces elevated levels of IL-6, IL-10 and IFNγ, but not TNFα in primary human microglial cells activated by LPS (Reiner et al., 2014). Although the precise explanation(s) for the observed selective effects on cytokines are unclear, these observations should not be too surprising given the complex role of cytokines in inflammation (Rathinam and Fitzgerald, 2016), coupled with the incomplete understanding of inflammatory regulation by CB_2 inverse agonists to date (Turcotte et al., 2016).

In addition to development as anti-inflammatory agents, CB_2 inverse agonists may represent a novel approach to treat certain forms of cancer (Feng et al., 2015). In support of this suggestion, there is significant overlap between the mechanisms by which RID-B and cannabinoids produce cytotoxicity in cancers of immune origin. For example, RID-B demonstrates anti-cancer activity in lymphoma and leukemia cancer cell lines that are both ER-positive and ER-negative (Nagahara et al., 2008). Mechanisms underlying the cytotoxic effect of RID-B in these cancer types include induction of apoptosis, activation of caspases-3, -8, and -9, and disruption of mitochondrial membrane potential. Similarly, the cannabinoids Δ^9-tetrahydrocannabinol (Δ^9-THC) and cannabidiol produce apoptosis of lymphoma and leukemia cell lines via disruption of mitochondrial membrane potential (Lombard et al., 2005; Mckallip et al., 2006). Furthermore, RID-B induces autophagy in the ER-negative Jurkat T-cell lymphoma cancer cell line, independent of the conventional Beclin 1 autophagy pathway (Nagahara et al., 2013). The cannabinoid WIN-55,212-2 also induces cell death via autophagy of non-Hodgkin lymphoma cells with no evidence of the traditional lysosomal degradation pathway (Wasik et al., 2011). Importantly, lymphoma and leukemia cell lines express little to no CB_1, but significant levels of CB_2 receptors (Mckallip et al., 2002; Lombard et al., 2005). Although not the primary focus of this study, it is interesting to note that high (10 μM), but not low (1 or 3 μM), concentrations of RID-B significantly decrease cell viability of LPS-activated macrophages via a cannabinoid receptor-dependent mechanism. Therefore, cytotoxic effects of RID-B reported in cancers of immune origin may be mediated via cannabinoid receptors and indicate an additional potential clinical use for this novel class of CB_2 inverse agonists.

An increasing body of literature suggests that tamoxifen does indeed exhibit significant anti-cancer action in cellular models of ER-negative breast cancer (reviewed in (Manna and Holz, 2016)). Although clinical cases reporting non-ER-mediated anti-cancer effects of tamoxifen are few, several have been noted. For example, a combination of tamoxifen with radiation increases overall survival of triple negative breast cancer patients when examined at 3-, 5- and 10-year post treatment (Payandeh et al., 2015). Furthermore, tamoxifen improves both drug response and survival of ER-negative and triple negative breast cancer patients in a manner that directly correlates to expression of estrogen-related receptor alpha (ERRalpha) (Manna et al., 2016) and androgen receptors (Hilborn et al., 2016). These clinical studies indicate that tamoxifen and carefully designed structural derivatives may one day be developed that exhibit clinical usefulness for treatment of non-ER expressing form of cancer, perhaps via CB_2 receptors.

Another important potential clinical use of CB_2 inverse agonists is treatment of osteoporosis, specifically due to reported anti-ostoeclastogenic effects of drugs in this class (Idris et al., 2005; Schuehly et al., 2011; Yang et al., 2013). Therefore, in the present study experiments were conducted to examine RID-B modulation of osteoclast differentiation from primary bone marrow macrophages (e.g., osteoclastogenesis). Bone integrity is maintained by bone remodeling wherein old bone is appropriately replaced with young matrix (Bhutani and Gupta, 2013). Osteoclasts are responsible for bone resorption while osteoblasts organize bone formation (Idris et al., 2005). Osteoporosis is a chronic disease characterized by decreased bone density and an increase risk of fractures, thought to be caused by an imbalance of bone remodeling. Treatment could therefore focus either on increasing bone

formation via activation of osteoblasts or decreasing bone resorption through decreasing formation/activity of osteoclasts (Bhutani and Gupta, 2013). CB_1 and CB_2 receptors are present in bone, and CB_2 inverse agonists produce significant decrease in the production of osteoclasts (Idris et al., 2005; Schuehly et al., 2011; Yang et al., 2013). For example, the selective CB_2 antagonist/inverse agonist AM-630 inhibits, while CB_2 agonists increase, osteoclast formation (Idris et al., 2008). Osteoclasts generated from CB_2 knockout are resistant to the anti-osteoclastogenic effects of AM-630, strongly supporting the argument that this effect is due to the CB_2 receptors (Idris et al., 2008). Similarly, a novel class of CB_2 selective inverse agonists derived from a triaryl sulfonamide scaffold produce potent inhibition of osteoclastogenesis (Yang et al., 2013). In this study, both CB_2 inverse agonists/antagonists examined, RID-B and AM-630, greatly reduced the number of osteoclasts formed and co-administration resulted in an additive effect. The cannabinoid agonist, CP-55,940 had little effect when administered alone, but produced almost complete antagonism with co-incubated with RID-B. Consequently, similar to that reported for other CB_2 inverse agonists, RID-B produces pronounced anti-osteoclastogenic effects that are likely mediated via cannabinoid receptors, and provides further evidence for potential use of drugs in this class for treatment of osteoporosis.

Although this and previous studies clearly demonstrate that SERM-scaffolds may be useful for synthesis of selective CB_1 and/or CB_2 cannabinoid ligands (Kumar and Song, 2013; Prather et al., 2013; Ford et al., 2016), before novel compounds can be useful therapeutically, drugs in this class must first be designed that lack ER affinity to prevent off-target effects. Importantly, RID-B is only a first generation of many ridaifen (RID) compounds that are tamoxifen derivatives, developed to reduce ER affinity, yet maintain cytotoxic effects in cancer (Shiina et al., 2008; Guo et al., 2013b). These studies have found that modification of substituents on the phenyl rings at the C1 position of tamoxifen greatly decrease affinity for ERα (Guo et al., 2013b). The structure of RID-B contains modifications of substituents associated with two phenyl rings. However, in order to completely lose affinity for ERα, one or both of the phenyl or ethyl groups at the C2 position must be eliminated. It is unknown how such modifications would alter the affinity of these compounds for cannabinoids receptors. Two RID compounds developed that completely lack ERα affinity have been investigated to determine ER-independent mechanism(s) of action for observed growth-inhibitory activity. The mechanism(s) of action observed for these compounds was poorly correlated to that of tamoxifen, indicating distinct cytotoxic modes of action for these two distinct classes of drugs (Guo et al., 2013b). For example, one of these compounds RID-SB8 exhibited broad cytotoxic effects across many human cancer cells lines with greater efficacy than tamoxifen. Characterization of the growth-inhibitory effects of RID-SB8 were shown to result from apoptosis, partially mediated via a caspase-independent pathway, alteration of AIF expression, and mitochondrial dysfunction (Guo et al., 2013a). Interestingly, the cannabinoid Δ^9-THC produces cytotoxicity in leukemia cells via similar mechanism(s) of action (Lombard et al., 2005). In summary, the tamoxifen derivative RID-B, developed to exhibit reduced affinity for ERs, acts as a high affinity selective CB_2 inverse agonist with anti-inflammatory, anti-osteoclastogenic and cytotoxic properties that are mediated by cannabinoid receptors. These

observations provide proof of principle for development of a novel class of SERM-based cannabinoids that act selectively at CB_2 and/or CB_1 receptors and lack affinity for ERs.

Acknowledgements

These studies were supported by bridging funds provided by the UAMS Department of Pharmacology and Toxicology and NIH/NIDA award no. DA039143 (PLP).

The osteoclast studies were made possible by Dr. Haibo Zhao's laboratory supported by NIH/NIAMS grants: AR062012 and AR068509.

Special thanks to Dr. Sung W. Rhee (Department of Pharmacology and Toxicology, University of Arkansas for Medical Sciences) for his assistance with microscopy and imaging.

Abbreviations:

AC	adenylyl cyclase
CB_1R	cannabinoid receptor type 1
CB_2R	cannabinoid receptor type 2
CHO	Chinese hamster ovary
CP-55,940	5-(1,1-dimethylheptyl)-2-[5-hydroxy-2-(3-hydroxypropyl)cyclohexyl]phenol
DMEM	Dulbecco's Modification of Eagle's Medium
ELISA	enzyme-linked immunosorbent assay
ER	estrogen receptor
GPCR	G-protein coupled receptor
[^{35}S]GTPγS	guanosine 5′-O-(3-[^{35}S]thio) triphosphate
hCB_2	human CB_2 receptors
IBMX	isobutyl-methyl-xanthine
RID	ridaifen
SERM	selective estrogen receptor modulator
TRAP	tartrate-resistant acid phosphatase
WIN-55,212-2	[(3R)-2,3-dihydro-5-methyl-3-(4-morpholinylmethyl)pyrrolo-[1,2,3-de]-1,4-benzoxazin-6-yl]-1-naphthalenyl-methanone

References

Alexander A, Smith PF, Rosengren RJ, 2009 Cannabinoids in the treatment of cancer. Cancer Lett. 285, 6–12. [PubMed: 19442435]

Bhutani G, Gupta MC, 2013 Emerging therapies for the treatment of osteoporosis. J. Midlife Health 4, 147–152. [PubMed: 24672186]

Bosier B, Muccioli GG, Hermans E, Lambert DM, 2010 Functionally selective cannabinoid receptor signalling: therapeutic implications and opportunities. Biochem. Pharmacol 80, 1–12. [PubMed: 20206137]

Bouaboula M, Perrachon S, Milligan L, Canat X, Rinaldi-Carmona M, Portier M, Barth F, Calandra B, Pecceu F, Lupker J, Maffrand JP, Le Fur G, Casellas P, 1997 A selective inverse agonist for central cannabinoid receptor inhibits mitogen-activated protein kinase activation stimulated by insulin or insulin-like growth factor 1. Evidence for a new model of receptor/ligand interactions. J. Biol. Chem 272, 22330–22339. [PubMed: 9268384]

Brailoiu GC, Deliu E, Marcu J, Hoffman NE, Console-Bram L, Zhao P, Madesh M, Abood ME, Brailoiu E, 2014 Differential activation of intracellular versus plasmalemmal CB2 cannabinoid receptors. Biochemistry (Mosc) 53, 4990–4999.

Cabral GA, Griffin-Thomas L, 2009 Emerging role of the cannabinoid receptor CB2 in immune regulation: therapeutic prospects for neuroinflammation. Expert Rev. Mol. Med 11, e3. [PubMed: 19152719]

Cabral GA, Rogers TJ, Lichtman AH, 2015 Turning over a new leaf: cannabinoid and endocannabinoid modulation of immune function. J. Neuro. lmmune Pharmacol. 10, 193–203.

Cheng Y, Prusoff W, 1973 Relationship between the inhibition constant (K1) and the concentration of inhibitor which causes 50 per cent inhibition (i50) of an enzymatic reaction. Biochem. Pharmacol 22, 3099–3108. [PubMed: 4202581]

Clark AJ, Lynch ME, Ware M, Beaulieu P, Mcgilveray IJ, Gourlay D, 2005 Guidelines for the use of cannabinoid compounds in chronic pain. Pain Res. Manag. 10 (Suppl. A), 44A–46A.

Coleman JW, 2001 Nitric oxide in immunity and inflammation. Int. Immunopharmacol 1, 1397–1406. [PubMed: 11515807]

Cosenza M, Gifford AN, Gatley SJ, Pyatt B, Liu Q, Makriyannis A, Volkow ND, 2000 Locomotor activity and occupancy of brain cannabinoid CB1 receptors by the antagonist/inverse agonist AM281. Synapse 38, 477–482. [PubMed: 11044895]

Dhopeshwarkar A, Mackie K, 2016 Functional selectivity of CB2 cannabinoid receptor ligands at a canonical and noncanonical pathway. J. Pharmacol. Exp. Ther 358, 342–351. [PubMed: 27194477]

Feng R, Tong Q, Xie Z, Cheng H, Wang L, Lentzsch S, Roodman GD, Xie XQ, 2015 Targeting cannabinoid receptor-2 pathway by phenylacetylamide suppresses the proliferation of human myeloma cells through mitotic dysregulation and cytoskeleton disruption. Mol. Carcinog 54, 1796–1806. [PubMed: 25640641]

Ford BM, Franks LN, Radominska-Pandya A, Prather PL, 2016 Tamoxifen isomers and metabolites exhibit distinct affinity and activity at cannabinoid receptors: potential scaffold for drug development. PLoS One 9, e0167240.

Garcia C, Palomo-Garo C, Garcia-Arencibia M, Ramos J, Pertwee R, Fernandez-Ruiz J, 2011 Symptom-relieving and neuroprotective effects of the phytocannabinoid Delta(9)-THCV in animal models of Parkinson's disease. Br. J. Pharmacol 163, 1495–1506. [PubMed: 21323909]

Goupil E, Laporte SA, Hebert TE, 2012 Functional selectivity in GPCR signaling: understanding the full spectrum of receptor conformations. Mini-Rev. Med. Chem 12 (9), 817–830. [PubMed: 22681252]

Grotenhermen F, Muller-Vahl K, 2012 The therapeutic potential of cannabis and cannabinoids. Dtsch Arztebl Int 109, 495–501. [PubMed: 23008748]

Guo WZ, Shiina I, Wang Y, Umeda E, Watanabe C, Uetake S, Ohashi Y, Yamori T, Dan S, 2013a Ridaifen-SB8, a novel tamoxifen derivative, induces apoptosis via reactive oxygen species-dependent signaling pathway. Biochem. Pharmacol 86, 1272–1284. [PubMed: 23973528]

Guo WZ, Wang Y, Umeda E, Shiina I, Dan S, Yamori T, 2013b Search for novel anti-tumor agents from ridaifens using JFCR39, a panel of human cancer cell lines. Biol. Pharm. Bull 36, 1008–1016. [PubMed: 23575219]

Hilborn E, Gacic J, Fomander T, Nordenskjold B, Stal O, Jansson A, 2016 Androgen receptor expression predicts beneficial tamoxifen response in oestrogen receptor-alpha-negative breast cancer. Br. J. Cancer 114, 248–255. [PubMed: 26742006]

Hojnik M, Dobovisek L, Knez Z, Ferk P, 2015 A synergistic interaction of 17-beta-estradiol with specific cannabinoid receptor type 2 antagonist/inverse agonist on proliferation activity in primary human osteoblasts. Biomed. Rep 3, 554–558. [PubMed: 26171165]

Holdsworth SR, Gan PY, 2015 Cytokines: names and numbers you should care about. Clin. J. Am. Soc. Nephrol 10, 2243–2254.

Idris AI, van't Hof RJ, Greig IR, Ridge SA, Baker D, Ross RA, Ralston SH, 2005 Regulation of bone mass, bone loss and osteoclast activity by cannabinoid receptors. Nat. Med 11, 774–779. [PubMed: 15908955]

Idris AI, Sophocleous A, Landao-Bassonga E, van't Hof RJ, Ralston SH, 2008 Regulation of bone mass, osteoclast function, and ovariectomy-induced bone loss by the type 2 cannabinoid receptor. Endocrinology 149, 5619–5626. [PubMed: 18635663]

Kenakin T, Miller LJ, 2010 Seven transmembrane receptors as shapeshifting proteins: the impact of allosteric modulation and functional selectivity on new drug discovery. Pharmacol. Rev 62, 265–304. [PubMed: 20392808]

Kumar P, Song ZH, 2013 Identification of raloxifene as a novel CB2 inverse agonist. Biochem. Biophys. Res. Commun 435, 76–81. [PubMed: 23611779]

Lombard C, Nagarkatti M, Nagarkatti PS, 2005 Targeting cannabinoid receptors to treat leukemia: role of cross-talk between extrinsic and intrinsic pathways in Delta9-tetrahydrocannabinol (THC)-induced apoptosis of Jurkat cells. Leuk. Res 29, 915–922. [PubMed: 15978942]

Lunn CA, Reich EP, Fine JS, Lavey B, Kozlowski JA, Hipkin RW, Lundell DJ, Bober L, 2008 Biology and therapeutic potential of cannabinoid CB2 receptor inverse agonists. Br. J. Pharmacol 153, 226–239. [PubMed: 17906679]

Maekawa T, Nojima H, Kuraishi Y, Aisaka K, 2006 The cannabinoid CB2 receptor inverse agonist JTE-907 suppresses spontaneous itch-associated responses of NC mice, a model of atopic dermatitis. Eur. J. Pharmacol 542, 179–183. [PubMed: 16824511]

Manna S, Holz MK, 2016 Tamoxifen action in ER-negative breast cancer. Sign. Transduct. Insights 5, 1–7. [PubMed: 26989346]

Manna S, Bostner J, Sun Y, Miller LD, Alayev A, Schwartz NS, Lager E, Fornander T, Nordenskjold B, Yu JJ, Stal O, Holz MK, 2016 ERRalpha is a marker of tamoxifen response and survival in triple-negative breast cancer. Clin. Cancer Res. 22, 1421–1431. [PubMed: 26542058]

Martinkovich S, Shah D, Planey SL, Arnott JA, 2014 Selective estrogen receptor modulators: tissue specificity and clinical utility. Clin. Interv. Aging 9, 1437–1452. [PubMed: 25210448]

Maximov PY, Lee TM, Jordan VC, 2013 The discovery and development of selective estrogen receptor modulators (SERMs) for clinical practice. Curr. Clin. Pharmacol 8, 135–155. [PubMed: 23062036]

Mckallip RJ, Lombard C, Fisher M, Martin BR, Ryu S, Grant S, Nagarkatti PS, Nagarkatti M, 2002 Targeting CB2 cannabinoid receptors as a novel therapy to treat malignant lymphoblastic disease. Blood 100, 627–634. [PubMed: 12091357]

Mckallip RJ, Jia W, Schlomer J, Warren JW, Nagarkatti PS, Nagarkatti M, 2006 Cannabidiol-induced apoptosis in human leukemia cells: a novel role of cannabidiol in the regulation of p22phox and Nox4 expression. Mol. Pharmacol 70, 897–908. [PubMed: 16754784]

Murataeva N, Mackie K, Straiker A, 2012 The CB2-preferring agonist JWH015 also potently and efficaciously activates CB1 in autaptic hippocampal neurons. Pharmacol. Res 66, 437–442. [PubMed: 22921769]

Nagahara Y, Shiina I, Nakata K, Sasaki A, Miyamoto T, Ikekita M, 2008 Induction of mitochondria-involved apoptosis in estrogen receptor-negative cells by a novel tamoxifen derivative, ridaifen-B. Cancer Sci. 99, 608–614. [PubMed: 18167132]

Nagahara Y, Takeyoshi M, Sakemoto S, Shiina I, Nakata K, Fujimori K, Wang Y, Umeda E, Watanabe C, Uetake S, Yamori T, Dan S, Yoshimi Y, Shinomiya T, Ikekita M, 2013 Novel tamoxifen derivative Ridaifen-B induces Bcl-2 independent autophagy without estrogen receptor involvement. Biochem. Biophys. Res. Commun 435, 657–663. [PubMed: 23688426]

Ouyang Q, Tong Q, Feng R, Myint KZ, Yang P, Xie XQ, 2013 Trisubstituted sulfonamides: a new chemotype for development of potent and selective CB2 receptor inverse agonists. ACS Med. Chem. Lett. 4, 387–392. [PubMed: 24729834]

Payandeh M, Sadeghi M, Sadeghi E, Aeinfar M, 2015 Clinicopathology figures and long-term effects of tamoxifen plus radiation on survival of women with invasive ductal carcinoma and triple negative breast cancer. Asian Pac. J. Cancer Prev. 16, 4863–4867. [PubMed: 26163605]

Pertwee RG, 2006 The pharmacology of cannabinoid receptors and their ligands: an overview. Int. J. Obes 30 (Suppl. 1), S13–S18.

Pertwee RG, 2010 Receptors and channels targeted by synthetic cannabinoid receptor agonists and antagonists. Curr. Med. Chem 17, 1360–1381. [PubMed: 20166927]

Poirier AA, Cote M, Bourque M, Morissette M, Di Paolo T, Soulet D, 2016 Neuroprotective and immunomodulatory effects of raloxifene in the myenteric plexus of a mouse model of Parkinson's disease. Neurobiol. Aging 48, 61–71. [PubMed: 27644075]

Prather PL, Francisdevaraj F, Dates CR, Greer AK, Bratton SM, Ford BM, Franks LN, Radominska-Pandya A, 2013 CB1 and CB2 receptors are novel molecular targets for Tamoxifen and 4OH-Tamoxifen. Biochem. Biophys. Res. Commun 441, 339–343. [PubMed: 24148245]

Presley C, Abidi A, Suryawanshi S, Mustafa S, Meibohm B, Moore BM, 2015a Preclinical evaluation of SMM-189, a cannabinoid receptor 2-specific inverse agonist. Pharmacol. Res. Perspect 3, e00159. [PubMed: 26196013]

Presley CS, Mustafa SM, Abidi AH, Moore BM II, 2015b Synthesis and biological evaluation of (3′, 5′-dichloro-2,6-dihydroxy-biphenyl-4-yl)-aryl/alkyl-methanone selective CB2 inverse agonist. Bioorg. Med. Chem 23, 5390–5401. [PubMed: 26275680]

Rathinam VA, Fitzgerald KA, 2016 Inflammasome complexes: emerging mechanisms and effector functions. Cell 165, 792–800. [PubMed: 27153493]

Reiner A, Heldt SA, Presley CS, Guley NH, Elberger AJ, Deng Y, D'Surney L, Rogers JT, Ferrell J, Bu W, Del Mar N, Honig MG, Gurley SN, Moore BM II, 2014 Motor, visual and emotional deficits in mice after closed-head mild traumatic brain injury are alleviated by the novel CB2 inverse agonist SMM-189. Int. J. Mol. Sci 16, 758–787. [PubMed: 25561230]

Rhee MH, Kim SK, 2002 SR144528 as inverse agonist of CB2 cannabinoid receptor. J. Vet. Sci 3, 179–184. [PubMed: 12514329]

Ross RA, Brockie HC, Stevenson LA, Murphy VL, Templeton F, Makriyannis A, Pertwee RG, 1999 Agonist-inverse agonist characterization at CB1 and CB2 cannabinoid receptors of L759633, L759656, and AM630. Br. J. Pharmacol 126, 665–672. [PubMed: 10188977]

Schuehly W, Paredes JM, Kleyer J, Huefner A, Anavi-Goffer S, Raduner S, Altmann KH, Gertsch J, 2011 Mechanisms of osteoclastogenesis inhibition by a novel class of biphenyl-type cannabinoid CB(2) receptor inverse agonists. Chem. Biol 18, 1053–1064. [PubMed: 21867920]

Shiina I, Sano Y, Nakata K, Kikuchi T, Sasaki A, Ikekita M, Nagahara Y, Hasome Y, Yamori T, Yamazaki K, 2008 Synthesis and pharmacological evaluation of the novel pseudo-symmetrical tamoxifen derivatives as anti-tumor agents. Biochem. Pharmacol 75, 1014–1026. [PubMed: 18177630]

Shoemaker JL, Joseph BK, Ruckle MB, Mayeux PR, Prather PL, 2005a The endocannabinoid noladin ether acts as a full agonist at human CB2 cannabinoid receptors. J. Pharmacol. Exp. Ther 314, 868–875. [PubMed: 15901805]

Shoemaker JL, Ruckle MB, Mayeux PR, Prather PL, 2005b Agonist-directed trafficking of response by endocannabinoids acting at CB2 receptors. J. Pharmacol. Exp. Ther 315, 828–838. [PubMed: 16081674]

Teixeira D, Marques C, Pestana D, Faria A, Norberto S, Calhau C, Monteiro R, 2016 Effects of xenoestrogens in human M1 and M2 macrophage migration, cytokine release, and estrogen-related signaling pathways. Environ. Toxicol 31, 1496–1509. [PubMed: 26011183]

Tsukuda S, Kusayanagi T, Umeda E, Watanabe C, Tosaki YT, Kamisuki S, Takeuchi T, Takakusagi Y, Shiina I, Sugawara F, 2013 Ridaifen B, a tamoxifen derivative, directly binds to Grb10 interacting GYF protein 2. Bioorg. Med. Chem 21, 311–320. [PubMed: 23199482]

Turcotte C, Blanchet MR, Laviolette M, Flamand N, 2016 The CB2 receptor and its role as a regulator of inflammation. Cell. Mol. Life Sci 73, 4449–4470. [PubMed: 27402121]

Ueda Y, Miyagawa N, Matsui T, Kaya T, Iwamura H, 2005 Involvement of cannabinoid CB(2) receptor-mediated response and efficacy of cannabinoid CB(2) receptor inverse agonist, JTE-907, in cutaneous inflammation in mice. Eur. J. Pharmacol 520, 164–171. [PubMed: 16153638]

Ueda Y, Miyagawa N, Wakitani K, 2007 Involvement of cannabinoid CB2 receptors in the IgE-mediated triphasic cutaneous reaction in mice. Life Sci. 80, 414–419. [PubMed: 17055000]

Valdeolivas S, Satta V, Pertwee RG, Fernandez-Ruiz J, Sagredo O, 2012 Sativex-like combination of phytocannabinoids is neuroprotective in malonate-lesioned rats, an inflammatory model of Huntington's disease: role of CB1 and CB2 receptors. ACS Chem. Neurosci. 3, 400–406. [PubMed: 22860209]

Vidinsky B, Gal P, Pilatova M, Vidova Z, Solar P, Varinska L, Ivanova L, Mojzis J, 2012 Anti-proliferative and anti-angiogenic effects of CB2R agonist (JWH-133) in non-small lung cancer cells (A549) and human umbilical vein endothelial cells: an in vitro investigation. Folia Biol. (Praha) 58, 75–80. [PubMed: 22578958]

Wasik AM, Almestrand S, Wang X, Hultenby K, Dackland AL, Andersson P, Kimby E, Christensson B, Sander B, 2011 WIN55,212-2 induces cytoplasmic vacuolation in apoptosis-resistant MCL cells. Cell Death Dis. 2, e225. [PubMed: 22048168]

Wilkerson JL, Gentry KR, Dengler EC, Wallace JA, Kerwin AA, Armijo LM, Kuhn MN, Thakur GA, Makriyannis A, Milligan ED, 2012 Intrathecal cannabilactone CB(2)R agonist, AM1710, controls pathological pain and restores basal cytokine levels. Pain 153, 1091–1106. [PubMed: 22425445]

Yang P, Wang L, Feng R, Almehizia AA, Tong Q, Myint KZ, Ouyang Q, Alqami MH, Wang L, Xie XQ, 2013 Novel triaryl sulfonamide derivatives as selective cannabinoid receptor 2 inverse agonists and osteoclast inhibitors: discovery, optimization, and biological evaluation. J. Med. Chem 56, 2045–2058. [PubMed: 23406429]

Yao BB, Mukherjee S, Fan Y, Garrison TR, Daza AV, Grayson GK, Hooker BA, Dart MJ, Sullivan JP, Meyer MD, 2006 In vitro pharmacological characterization of AM1241: a protean agonist at the cannabinoid CB(2) receptor? Br. J. Pharmacol 153 (2), 390–401.

Yazgan B, Yazgan Y, Ovey IS, Naziroglu M, 2016 Raloxifene and tamoxifen reduce PARP activity, cytokine and oxidative stress levels in the brain and blood of ovariectomized rats. J. Mol. Neurosci 60, 214–222. [PubMed: 27372663]

Zhou J, Fujiwara T, Ye S, Li X, Zhao H, 2015 Ubiquitin E3 ligase LNX2 is critical for osteoclastogenesis in vitro by regulating M-CSF/RANKL signaling and Notch2. Calcif. Tissue Int. 96, 465–475. [PubMed: 25712254]

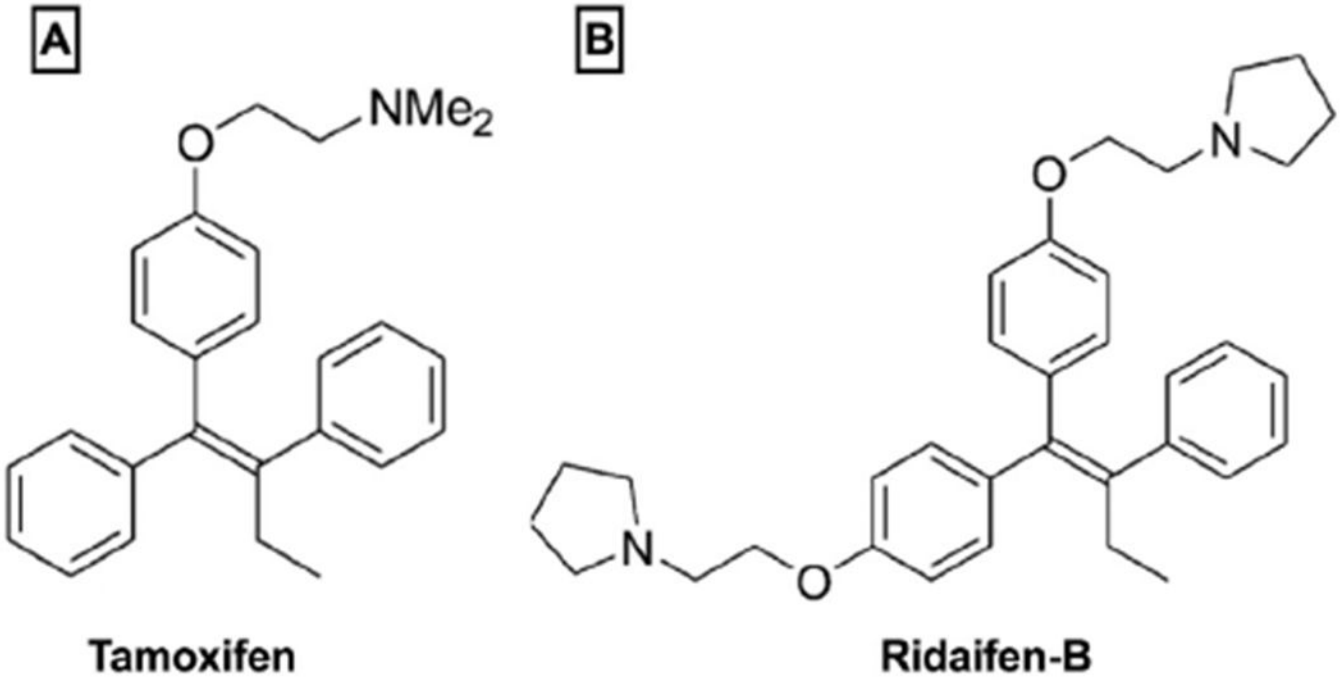

Fig. 1.

Structures of ligands examined in this study. The ligands examined in this study were; A) tamoxifen, classified as a selective estrogen receptor modulator (SERM) in the triphenylethylene structural class (Maximov et al., 2013), recently shown to also exhibit moderate affinity for CE_1 and CB_2 receptors (Prather et al., 2013); and B) ridaifen-B, a pseudo-symmetrical derivative of tamoxifen developed to exhibit reduced affinity for estrogen receptors (ERs) while maintaining cytotoxic actions in cancer models (Shiina et al., 2008).

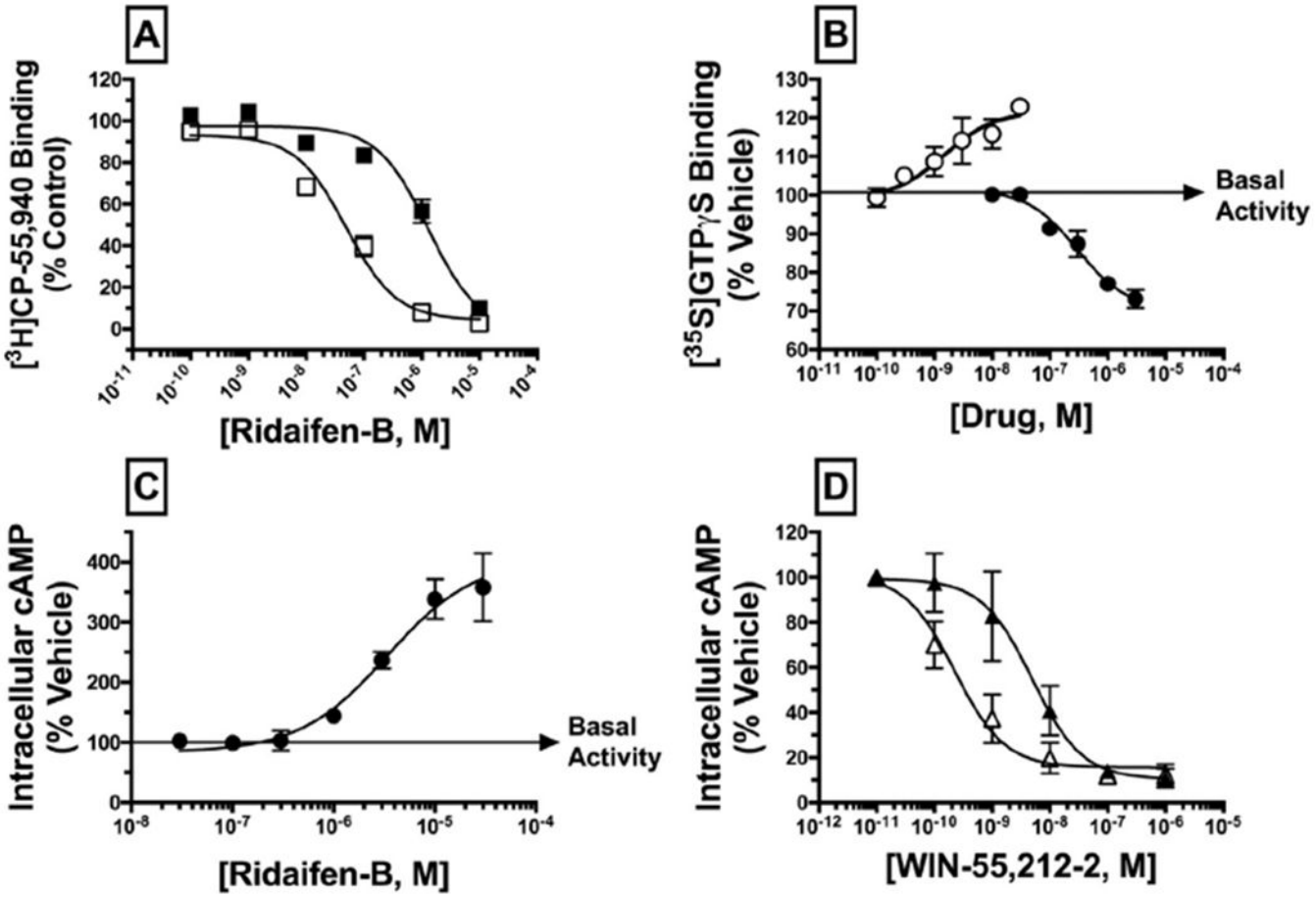

Fig. 2.

RID-B acts as a high-affinity, CB_2 selective antagonist/inverse agonist. A) IC_{50} values for competition between increasing concentrations of RID-B (10^{-10} to 10^{-5} M) and 0.2 nM of [^{3}H]-CP-55,940 were determined experimentally by incubation with 50 μg of membranes prepared from CHO-hCB_1 cells (filled squares) or CHO-hCB2 cells (open squares). As a quantitative measure of affinity, K_i values were calculated using experimental IC_{50} values by employing the Cheng Prusoff equation (Cheng and Prusoff, 1973). RID-B demonstrates 17-fold selectivity for binding to CB_2 relative to CB_1 receptors. B) Modulation of G-protein activity was examined by incubating 0.1 nM of the non-hydrolyzable [^{35}S]GTPγS analogue with increasing concentrations of RID-B (10^{-8} to 10^{-5}M; filled circles) or CP-55,940 (10^{-10} to 10^{-7} M; open circles) and 25 μg of CHO-hCB_2 membrane. CP-55,940 increases G-protein binding, indicative of agonist activity, while RID-B decreases G-protein binding, indicative of inverse agonist activity. C) Modulation of forskolin-stimulated adenylyl cyclase activity was examined by incubating CHO-hCB_2 cells with increasing concentrations of RID-B (10^{-8} to 10^{-4}M) as described in the Materials and Methods section. D) Inhibition of adenylyl cyclase activity by the CB_1/CB_2 agonist WIN-55,212-2 alone (open triangles) or in the presence of a receptor saturating concentration of RID-B (3 μM; filled triangles) was examined in CHO-hCB_2 cells. Potency (EC_{50} or IC_{50}) and efficacy (E_{max} or I_{max}) values for all curves presented in panels A-D were derived from non-linear regression analysis.

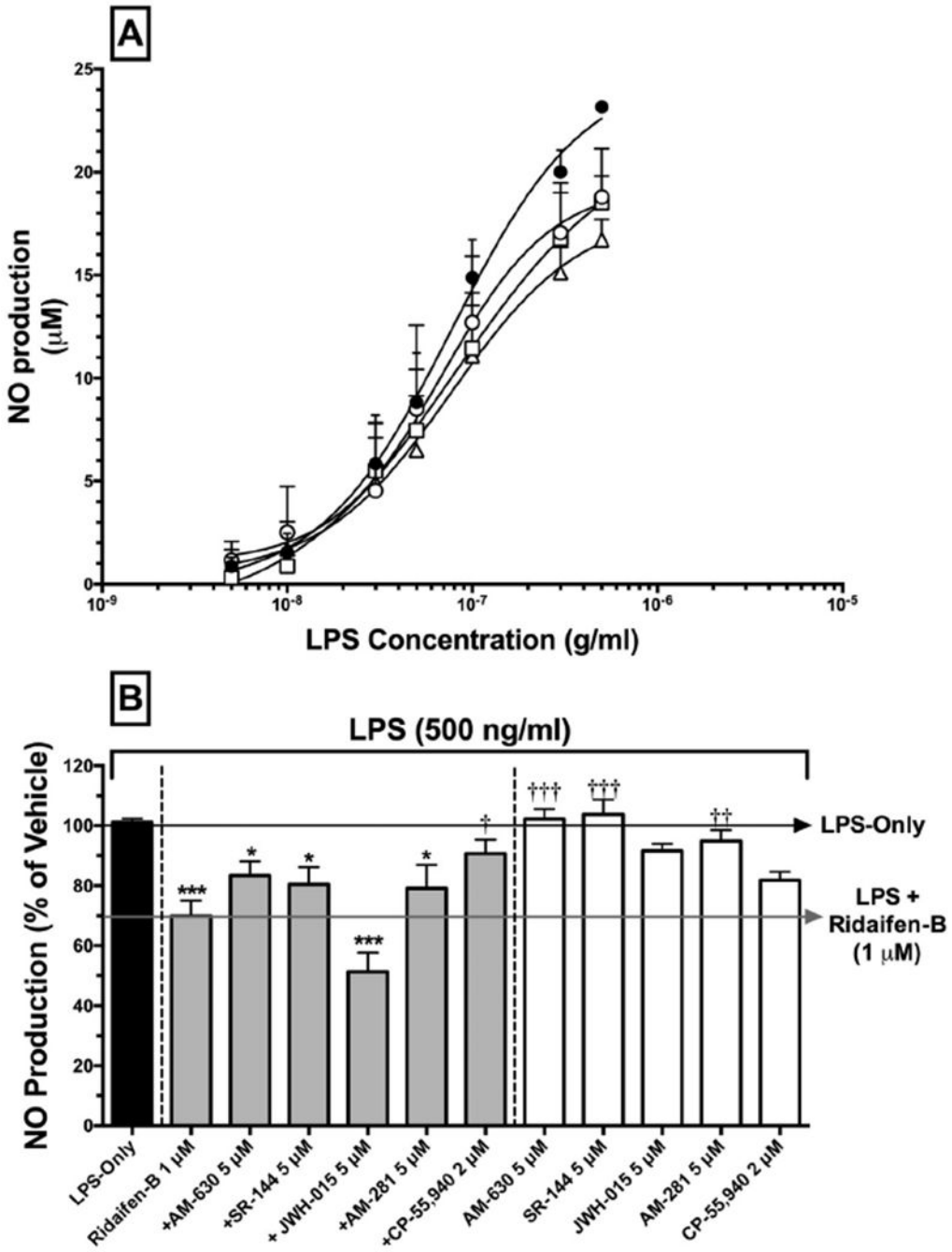

Fig. 3.

RID-B reduces NO production in LPS-stimulated RAW 264.7 macrophages in a cannabinoid-dependent manner. A) RAW 264.7 macrophages were incubated with LPS-alone (filled circles), LPS + 300 nM (open circles), LPS + 500 nM (open squares), or LPS + 1 μM of RID-B (open triangles) for 48 h. Supernatants were analyzed for presence of nitrite using the Greiss reagent. Data represent the mean ± SEM for 3–5 experiments conducted in triplicate. B) RAW 264.7 macrophages were treated with LPS-alone (black bar), LPS + RID-B alone, LPS + RID-B plus cannabinoids acting via CB_1 and/or CB_2

receptors (gray bars), or LPS with cannabinoids alone (white bars). Statistical analysis to determine differences between treatments employed a one-way ANOVA with Dunnett's multiple comparison *post-hoc* test. Asterisks denote statistically significant differences from vehicle-treated cells (*$p < 0.05$, **$p < 0.01$, ***$p < 0.001$). Crosses signify statistical differences from RID-B 1 μM treatment. ($^{\dagger}p < 0.05$, $^{\dagger\dagger}p < 0.01$, $^{\dagger\dagger\dagger}p < 0.001$).

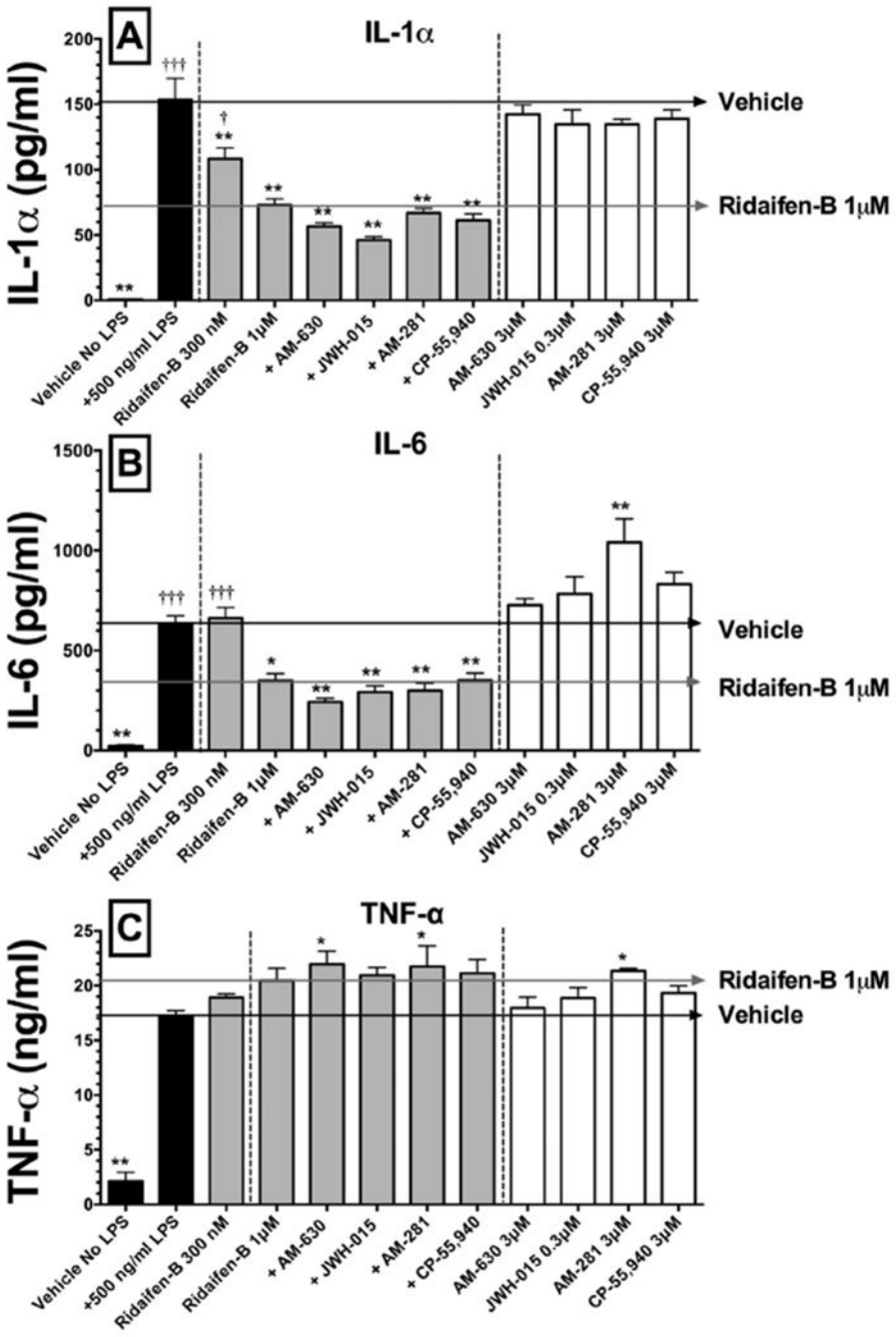

Fig. 4.

The effect of RID-B on IL-1α, IL-6, and TNFα release in LPS-stimulated RAW 264.7 macrophages. Black bars represent IL-1α (panel A), IL-6 (panel B) or TNFα (panel C) release in the absence (left) or presence (right) of LPS (500 ng for 48 h). Gray Bars represent RID-B alone (300 nM) or plus co-incubation of cannabinoids acting via CB_1 and/or CB_2 receptors, while white bars represent incubation with cannabinoids alone. Cytokines levels were measured by ELISA. The results are expressed as the mean ± SEM for separate experiments conducted in triplicate. Asterisks denote values significantly

different from macrophages treated with LPS 500 ng/ml (*p < 0.05, **p < 0.01, ***p < 0.001, using a one-way ANOVA followed by a Dunnett's multiple comparison *post-hoc* test). Crosses represent statistically significant values from treatment with RID-B 1 μM.

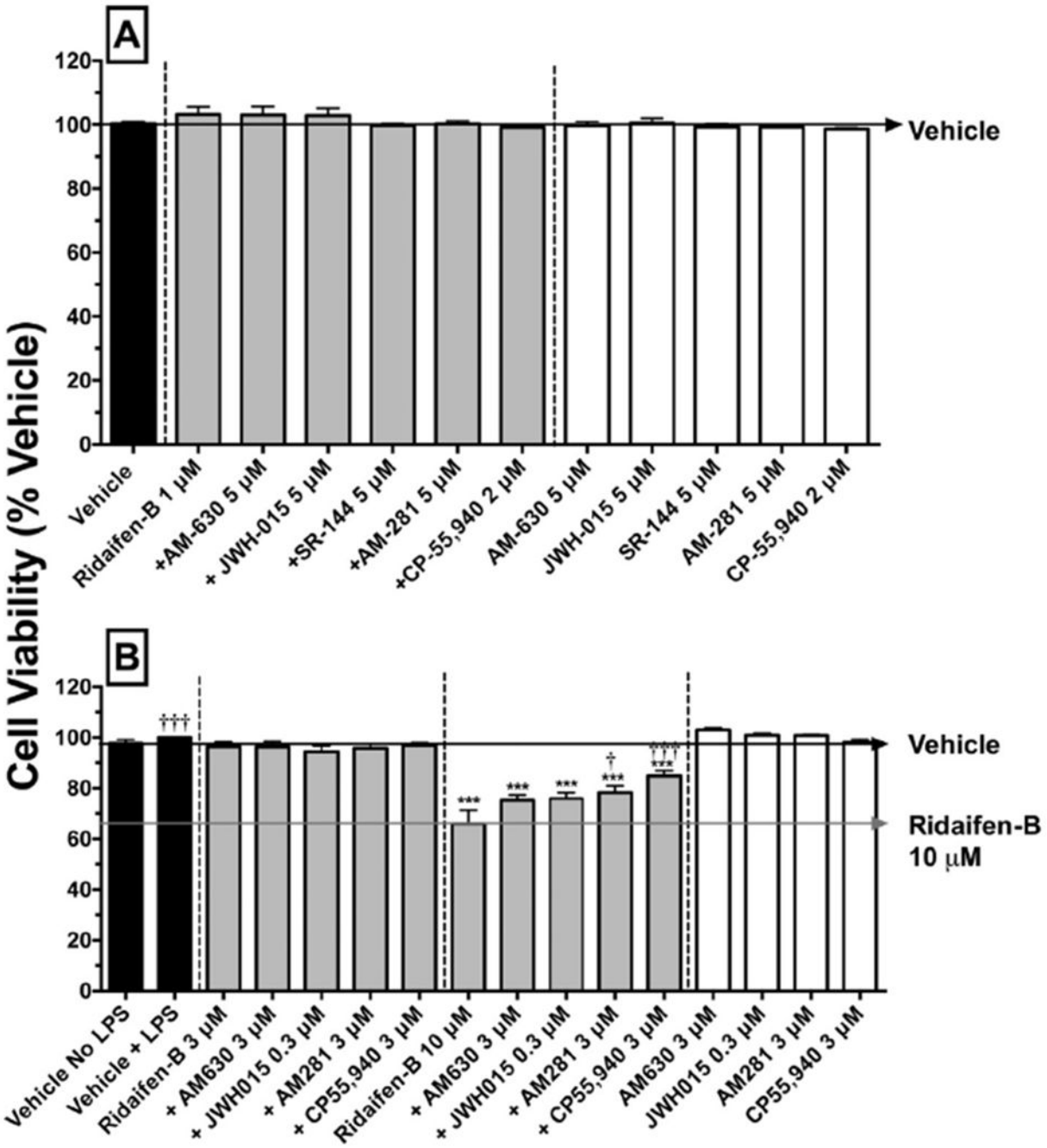

Fig. 5.

High but not low concentrations of RID-B reduce cell viability of LPS-stimulated RAW 264.7 macrophages in a cannabinoid-dependent manner. Cell viability was analyzed by using the WST-1 reagent 4 (panel A) and 48 (panel B) hours after addition of LPS (500 ng/ml). Results represent the mean ± SEM of independent experiments conducted from 4 to 12 times in triplicate. LPS-stimulated macrophages were treated with vehicle (black bars), RID-B alone, RID-B plus cannabinoids acting via CB_1 and/or CB_2 receptors (gray bars), or with cannabinoids alone (white bars). Statistical analysis to determine differences between

treatments employed a one-way ANOVA with Dunnett's multiple comparison *post-hoc* test. Asterisks denote values significantly different from vehicle-treated macrophages (*$p < 0.05$, **$p < 0.01$, ***$p < 0.001$, using a one-way ANOVA with Dunnett's multiple comparison *post-hoc* test). Crosses represent values statistically different from treatment with RID-B 10 μM ($^{\dagger}p < 0.05$, $^{\dagger\dagger\dagger}p < 0.001$, using a one-way ANOVA with Dunnett's multiple comparison *post-hoc* test).

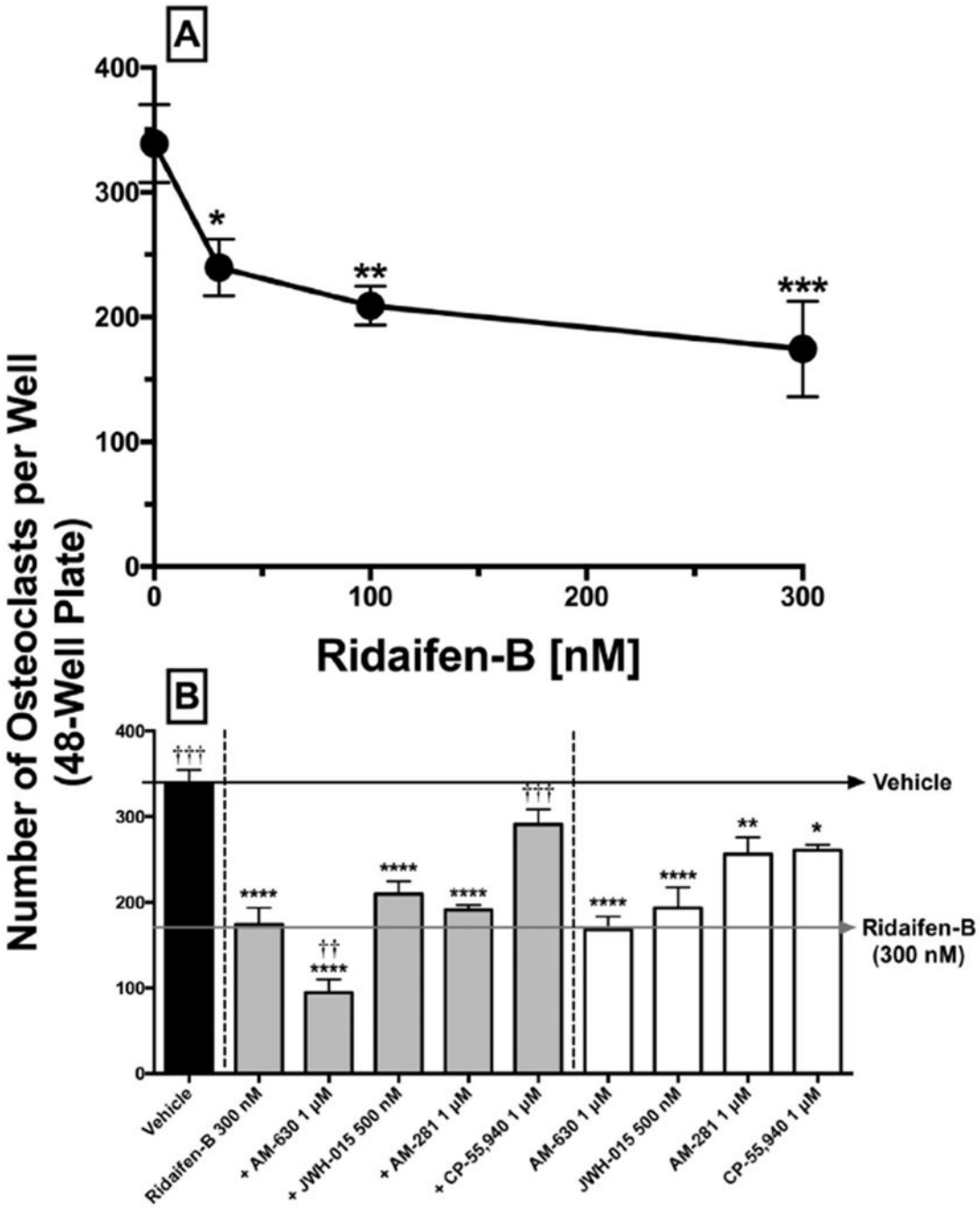

Fig. 6.

RID-B reduces osteoclast formation in a concentration- and cannabinoid-dependent manner. A) Pre-osteoclasts were incubated with 30 nM, 100 nM, and 300 nM of RID-B. B) Black bars represent osteoclasts formed in the presence of vehicle only. Gray bars represent osteoclastogenesis in the presence of RID-B or RID-B plus cannabinoids acting via CB_1 and/or CB_2 receptors (gray bars), or with cannabinoids alone (white bars). Osteoclasts were quantified visually by microscopy using a grid system. Osteoclasts were cultured from wild-type mouse bone marrow macrophages using M-CSF and RANK-L for 4 days. Drugs were

added on days 2 and 3. Four independent experiments were conducted in triplicate. Results represent means ± SEM. Statistical analysis to determine differences between treatments employed a one-way ANOVA with Dunnett's multiple comparison *post-hoc* test. Values statistically different from vehicle treatment are noted with asterisks (*$p < 0.05$, **$p < 0.01$, ***$p < 0.001$). Values significantly differing from RID-B 300 nM treatment are indicated by crosses ($^{\dagger}p < 0.05$, $^{\dagger\dagger}p < 0.01$, $^{\dagger\dagger\dagger}p < 0.001$).

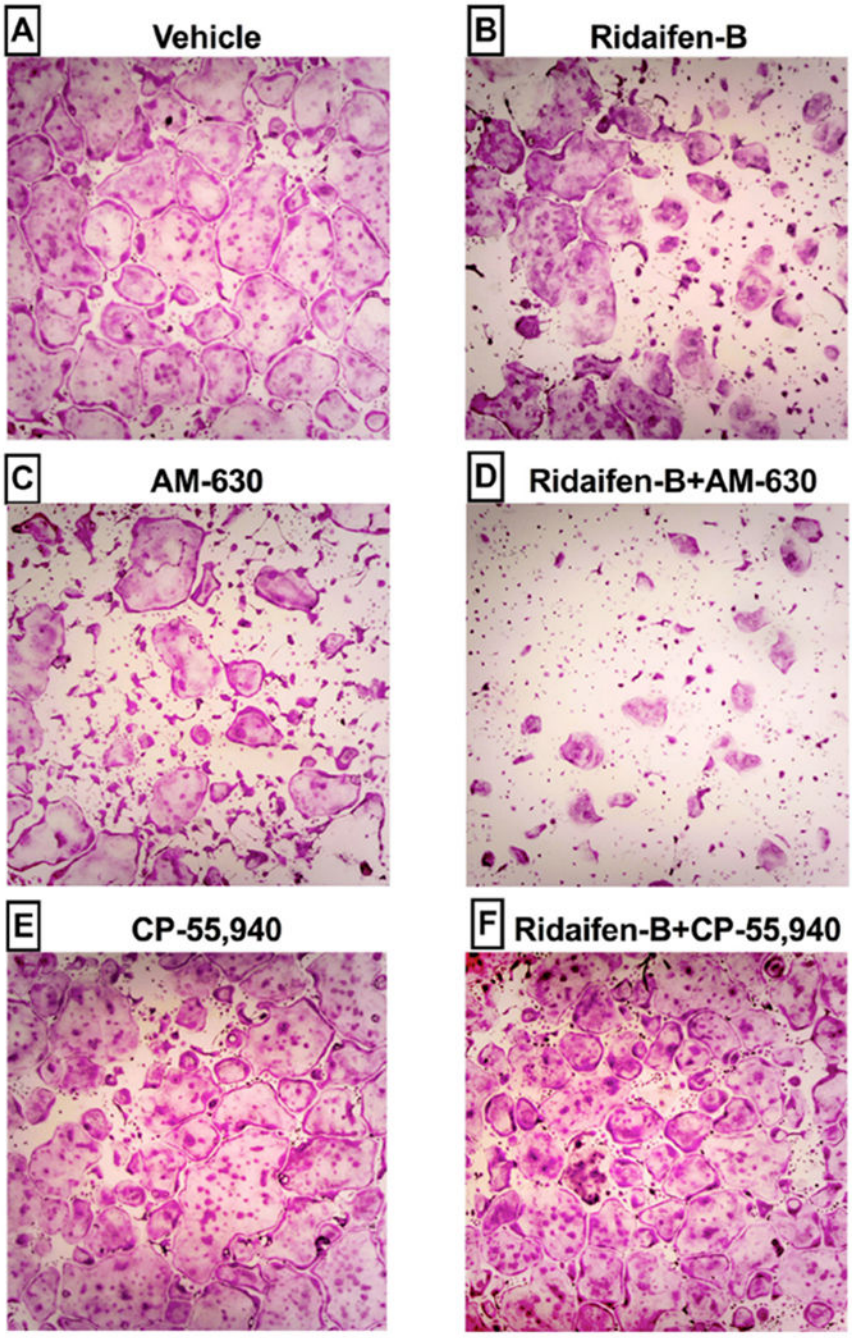

Fig. 7.

Anti-osteoclastogenic effects are produced by the CB_2 inverse agonist RID-B are attenuated by co-incubation with CB_1/CB_2 agonist CP-55,940. Tartrate-resistant acid phosphatase (TRAP) staining of wild-type osteoclasts, cultured for 4 days in a 48 well plate in the presence of A) vehicle, B) RID-B (300 nM), C) AM-630 (1 μM), D) RID-B (300 nM) + AM-630 (1 μM), E) CP-55,940 (1 μM) or F) RID-B (300 nM) + CP-55,940 (1 μM) are

presented. Images are representative of those taken from four independent experiments conducted in triplicate.